Springer

KSME

Journal of Mechanical Science and Technology 31 (8) (2017) 4051~4059
www.springerlink.com/content/1738-494x(Print)/1976-3824(Online)
DOI 10.1007/s12206-017-0753-5

Performance optimization of diesel engine fueled with diesel–jatropha curcas biodiesel blend using response surface methodology †

Huaping Xu[1,2], Bifeng Yin[1,*], Shengji Liu[1] and Hekun Jia[1]

[1]*School of Automobile and Traffic Engineering, Jiangsu University, Zhenjiang 212013, China*
[2]*School of Energy and Power Engineering, Jiangsu University of Science and Technology, Zhenjiang 212003, China*

(Manuscript Received February 13, 2017; Revised April 10, 2017; Accepted April 21, 2017)

Abstract

The present work is aimed at unfolding the effect of fuel supply parameters such as Fuel injection pressure (FIP), Start of injection timing (SOI), Pilot-main injection intervals (PMII) on performance and emission characteristics of 20 % blend of Jatropha curcas biodiesel (J20) under light load operation of a diesel engine. The experiments were designed using design of experiments based on the fractional factorial design of Response surface methodology (RSM). Multiple regression models developed using RSM for measured responses like nitrogen oxides (NO_X), SOOT, hydrocarbon (HC), Brake specific fuel consumption (BSFC) and Brake thermal efficiency (BTE), were found to be statistically significant by Analysis of variance (ANOVA). Interactive effects among FIP, SOI and PMII were analyzed using response surface graphs that were fitted using developed RSM models. Optimization was performed using the desirability approach of the RSM for lesser emissions and BSFC simultaneously with superior BTE. A FIP of 134.11 MPa, SOI of 6.4 BTDC, and PMII of 5.8 CA were found to be optimal values for J20 in the test engine of 21 kW at 1800 rpm. The results of this study show that at optimal input parameters, the values of the NO_X, SOOT, HC, BSFC and BTE with a high desirability of 96.7 % are 603.44 ppm, 0.037 FSN, 12.73 ppm, 233.26 g/kW h and 37.31 %, respectively.

Keywords: Biodiesel; Response surface methodology; Experiment design; Diesel engine; Emissions

1. Introduction

The increasingly stricter exhaust emission regulation and the danger of fossil fuels depletion propelled the application of renewable sources. Among the renewable alternatives, biodiesels have attracted more attention as alternatives to diesel engine fuels. The newly released proposed regulations by the US Environmental Protection Agency (EPA) for the 2014–2017 Renewable fuel standard (RFS) requires a significant rising for biodiesels ranging from 1.63 to 1.90 billion gallons yearly [1]. In the "Directive EC 2003/96", the European Union rules that the blending ratio fossil diesel and biodiesel much be greater than 5.75 % [2]. Generally, biodiesels are produced via triglyceride transesterification from plant vegetable oils and used cooking oils or animal fats [3-5]. The advantages of biodiesels, besides their environmental friendliness and renewability, are their higher cetane number and lower sulfur, enhanced lubrication properties and higher biodegradability [6, 7].

During the last decade, biodiesels have been widespread investigated in various diesel engines [8-10]. Many valuable researches have been conducted on the effect of biodiesels on exhaust emissions and performance compared to fossil diesel [11, 12]. Hwaichyuan et al. [13], using crude Calophyllum inophyllum oil, found the biodiesel to be effective in reducing fuel consumption, carbon monoxide (CO) and smoke emissions, while slightly increasing oxides of nitrogen (NO_X) emissions. Cheik et al. [14] investigated the effects of engine load and speed on emissions using biodiesel blends. They found that Particulate matter (PM) and CO emissions were extremely related to engine load, while Unburned hydrocarbon (UHC) emissions increased with engine speed.

Since biodiesels have some physicochemical properties different from conventional diesel, it is important to research the influence of various fuel supply parameters on emission characteristics and economy of biodiesels. Jeon et al. [7] conducted an experimental study on an optical CI engine fueled with biodiesel. Lower flame temperature was observed as the pilot fuel mass increased. Deshmukh et al. [15] reported that straight vegetable oils had longer injection delays at low injection pressures. They attributed this phenomenon to their higher viscosity. Torres et al. [16] examined the impact of biodiesel on various injection system parameters, such as maximum injection pressure and injection duration, and injec-

*Corresponding author. Tel.: +86 511 88797620, Fax.: +86 511 88797620
E-mail address: ybf@ujs.edu.cn
† Recommended by Associate Editor Jeong Park

Table 1. Property of Jatropha curcas oil and diesel.

Property	Unit	Jatropha curcas	0# diesel
Density at 20 °C	kg/mm^3	912	839
Lower heating value	MJ/kg	37.55	42.5
Kinematic viscosity at 40 °C	mm^2/s	33.490	3.048
Cetane number		51	40-55
Flash point	°C	279	67

Table 2. Engine main technical data.

Engine type	In-line 4 cylinders
Bore/stroke	102 mm/118 mm
Compression ratio	17
Displacement	3857 cc
Fuel injection system	Bosch common rail
Rated power	105kW@2800 rpm

tion timing.

The common testing of the diesel engine for biodiesel-diesel blends under all possible operating conditions of varying injection parameters is both time consuming and expensive [17-19]. As a feasible substitute, engine performance and emissions can be modeled using Response surface methodology (RSM) [20]. RSM is a collection of statistical and mathematical techniques applied in the progression of a proper functional relationship between the response and the input parameters. Dhole et al. [21] developed mathematical models to relate the brake thermal efficiency, Unburnt hydrocarbons (UHC), CO and NO_X by varying engine parameters like Load and H2 fuel substitution using RSM. Lee et al. [22] performed optimization of the fuel injection control of diesel engines using RSM, and found that NO_X and PM emissions can be reduced simultaneously while no substantial increase in fuel consumption. Jagannath et al. [18] optimized a single cylinder diesel engine with respect to brake power, fuel economy and smoke emissions through experimental investigation and RSM.

The purpose of this study was focused on the performance and emissions analysis of diesel engine on 20 % blend of Jatropha curcas biodiesel (J20) with different injection strategies. RSM and desirability function were employed to optimize the fuel supply parameters (FIP, SOI and PMII) which would be resulting in improved performance with lesser emissions.

2. Experimental setup and procedure

2.1 Fuel properties

While studies have mostly shown SOOT decrease for higher ratio biodiesel blends, it is equally true that the fuel consumption is higher than diesel, especially mixing ratio more than 20 % [8]. Hence, the Jatropha curcas biodiesel blend (80 % diesel and 20 % jatropha curcas oil by volume, named J20) was employed in this study. Blending was performed by a blending machine at 4000 rpm for 25-30 min. The general properties of Jatropha curcas, 0# diesel are shown in Table 1.

2.2 Engine test bench

The experiments were on a four-cylinder, water-cooled, turbocharged diesel engine. Test engine specifications are reported in Table 2, and a schematic of the experimental setup is

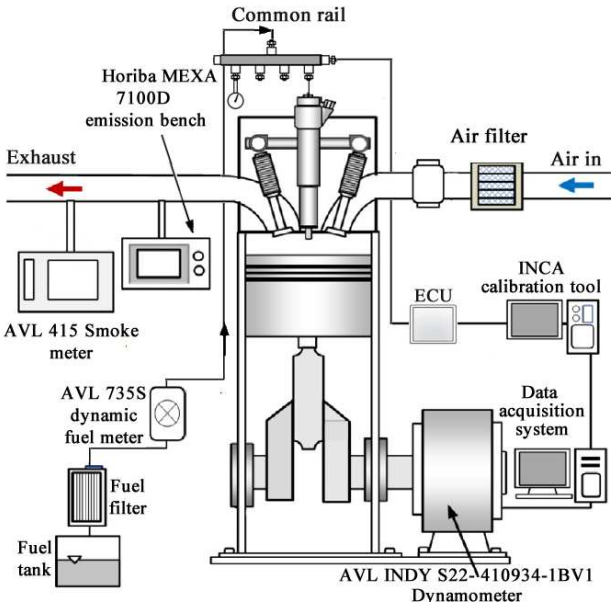

Fig. 1. Schematic diagram of experimental system.

shown in Fig. 1. To control the load and speed of the diesel engine, AC dynamometer (AVL INDYS22-410934-1BV-1) was connected to the engine. The fuel injection parameters were controlled by a Bosch common rail direct injection system, and a gravimetric fuel flow-meter (AVL 735S) was equipped. FIP, PMII and SOI timing were controlled using INCA based Engine management system (EMS), which has flexibility for user defined control of various fuel injection parameters. The experiments were carried out for 25 % of load (21 kW) at a speed of 1800 rpm. All pilot injection quantity was 3 mg.

An emission analyzer (HORIBA MEXA 7100D) was used to measure HC, CO and NO_X in the exhaust. The measuring principle of HC was the hydrogen flame ionization detection method, while CO was measured via the nondispersive infrared method. And the chemiluminescent method was adopted to quantify NO_X emission. Furthermore, a filter paper smoke meter (AVL 415) was used to measure the Filter smoke number (FSN).

2.3 Experimental design

We applied RSM for the experimental design and optimization with the software Design Expert (trial version 8.0.5, Stat-Ease). Fractional factorial design was employed for RSM in

Table 3. The range and level of the independent parameters.

Independent variable	Range and level		
	-1	0	1
FIP (MPa)	110	125	140
SOI (BTDC)	1.5	6.5	11.5
PMII (CA)	1	6	11

the experimental design. Three experiment parameters, including the Fuel injection pressure (FIP), the Start of injection timing (SOI), and the Pilot-main injection intervals (PMII), were selected as independent parameters on the exhaust emissions, NO_X (ppm), SOOT (FSN), HC (ppm), as well as BSFC (g/kW h) and BTE (%) as responses. The experimental design consisted of 80 runs and the experimental range and level of the process independent parameters determined in preliminary experiments are given in Table 3.

The relationship between the input parameters and each response could be depicted as a second-degree polynomial quadratic equation [23]:

$$Y = b_0 + \sum_{i=1}^{k} b_i x_i + \sum_{i=1}^{k} b_{ii} x_i^2 + \sum_{i=1, j=i+1}^{k} b_{ij} x_i x_{ij} + \varepsilon , \quad (1)$$

where Y is the response, b_0 is the model constant, k is the number of input parameters studied, b_i is the regression coefficients of the individual linear effect, b_{ii} is the quadratic effect, b_{ij} is the interaction between the input parameters, while x_i and x_{ij} are the input parameters, and ε is the error.

3. Desirability approach and anova analysis

3.1 Desirability approach

In this work, the multi-response optimization was conducted using design expert software. The desirability function is one of the most important multi-target optimization methods in mathematics. This methodology is based on constructing a desirability function for each response, where each response is transformed to a dimensionless individual desirability (d_i) scale. The scale of the individual desirability function ranges between d = 0, which suggests that the response is completely unacceptable, and d = 1 suggests that the response is more desirable [18].

Because the target of most responses in this study was to be minimized, thus the individual desirability (d_i) is described according the following equation [24]:

$$d_i = \begin{cases} 1 \ \ if \ Y_i > H_i \\ \left(\dfrac{Y_i - L_i}{H_i - L_i} \right)^s \ \ if \ L_i \le Y_i \le H_i , \\ 0 \ \ if \ Y_i < H_i \end{cases} \quad (2)$$

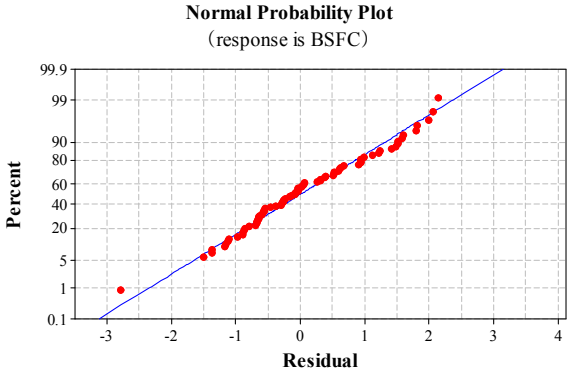

Fig. 2. Normal probability plot of the residual for the composite for response of BSFC.

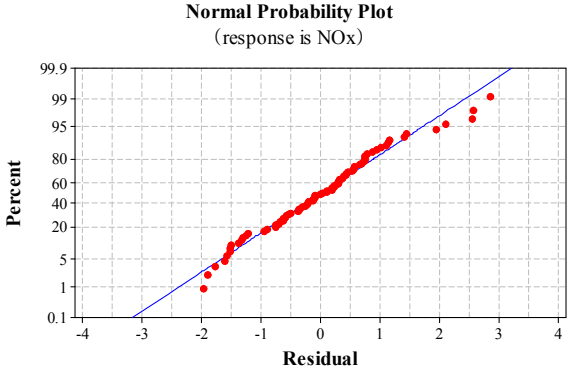

Fig. 3. Normal probability plot of the residual for the composite for response of NO_X.

where i indicates the response, Y is the value of each response, L and H are the lower and upper limit of the response, respectively. And s is the weight of the response.

With the individual desirability, it is then possible to obtain the overall Desirability (D). The overall desirability function D is defined as the weighted geometric average of the individual desirability (d_i) according the following equation [25]:

$$D = \sqrt[m]{d_1 d_2 d_3 \ldots d_m}, \quad (3)$$

where m is the number of responses studied in the optimization process. Thus, the simultaneous optimization process is reduced to find the level of factors that demonstrate the maximum D.

3.2 ANOVA analysis

The experimentation responses of all 80 runs were analyzed by RSM. The corresponding response surface equations were established by regressive analysis and then tested by Analysis of variance (ANOVA) to evaluate the accuracy. Figs. 2-4 show the normal probability plots of BSFC, NO_X and SOOT, respectively. The residuals in each plot generate near the straight line, which means the errors are distributed normally

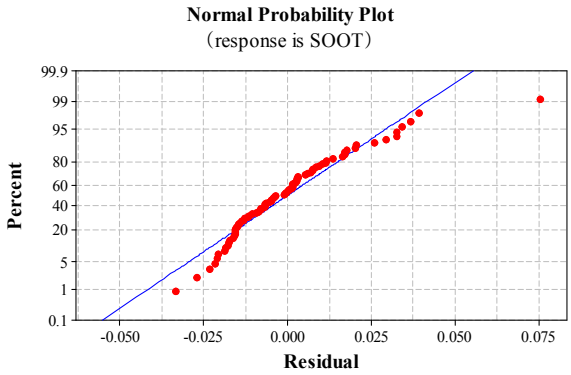

Fig. 4. Normal probability plot of the residual for the composite for response of SOOT.

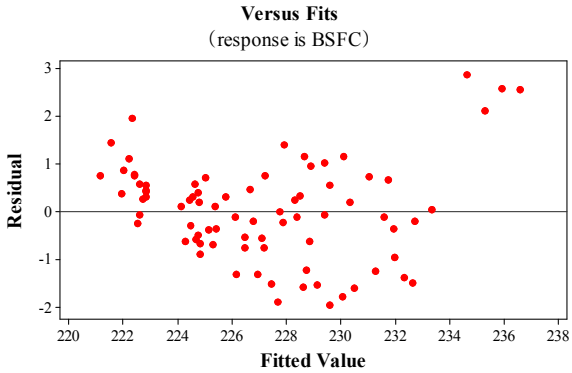

Fig. 5. Residual versus fitted line of the composites for the corresponding responses of BSFC.

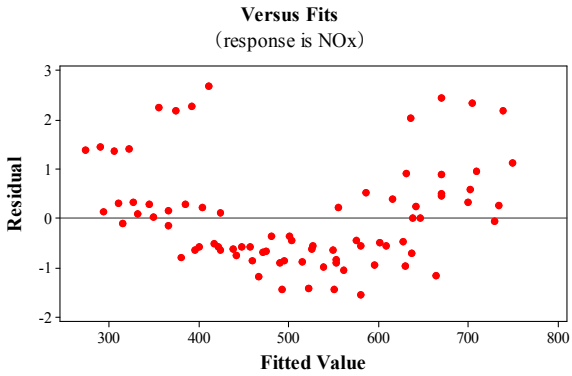

Fig. 6. Residual versus fitted line of the composites for the corresponding responses of NO_X.

[20]. Meanwhile, the residual plots versus fitted line for each response are shown in Figs. 5-7. The residuals are independently distributed with zero mean and a constant variance. The rest of the responses were also analyzed, their models were adequate and satisfied as well.

The ANOVA for the input parameters is given in Table 4; the significance of the input parameter over the output responses as the p value was less than 0.05 [26, 27]; the model was significant with p values less than 0.0001. The regression statistics goodness of fit (R^2) and the goodness of prediction

Table 4. Analysis of variance for responses (values of "p").

Source	NO_X	SOOT	HC	BSFC	BTE
Model	< 0.0001	< 0.0001	< 0.0001	< 0.0001	< 0.0001
FIP	0.0296	< 0.0001	< 0.0001	0.6356	0.9508
SOI	< 0.0001	< 0.0001	< 0.0001	0.0072	< 0.0001
PMII	0.0031	0.0007	0.8311	0.2284	0.0051
FIP*SOI	0.0028	0.2361	0.0092	0.0381	0.8570
FIP*PMII	0.2242	< 0.0001	0.1696	0.5447	0.0402
SOI*PMII	< 0.0001	0.4321	0.0048	< 0.0001	< 0.0001
FIP^2	0.2359	0.3726	0.1648	0.5822	< 0.0001
SOI^2	< 0.0001	0.2728	0.9950	< 0.0001	0.2884
$PMII^2$	0.8366	< 0.0001	< 0.0001	< 0.0001	0.0024

Table 5. Response surface model evaluation.

Model	NO_X	SOOT	HC	BSFC	BTE
Mean	511.46 ppm	0.050 FSN	14.85 ppm	237.37 g/kW h	0.37 %
Std.Dev	19.02	0.013	0.016	1.51	0.0001
R^2	0.9819	0.9656	0.9512	0.8941	0.9551
Adj. R^2	0.9796	0.9731	0.9678	0.8805	0.9409
Pred. R^2	0.9748	0.9843	0.9753	0.8596	0.9168

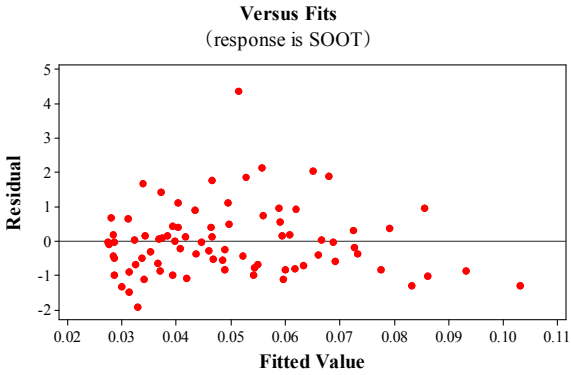

Fig. 7. Residual versus fitted line of the composites for the corresponding responses of SOOT.

(Adjusted R^2) are described in Table 5. The R^2 value signifies the total variability of response after considering the significant factors and the Adjusted R^2 value accounts for the number of predictors in the model [28]. It is obvious that the values indicate that the model fits the data fairly well.

4. Results and discussion

4.1 NO_X emissions

The response surface quadratic model of NO_X emissions in terms of the experimental results was given as Eq. (4):

$$NO_X = -249.48 + 8.56FIP - 7.37SOI - 0.29PMII + 0.16FIP*SOI - 0.06FIP*PMII + 0.81SOI*PMII - 0.02FIP^2 + 2.09SOI^2 + 0.04PMII^2 . \quad (4)$$

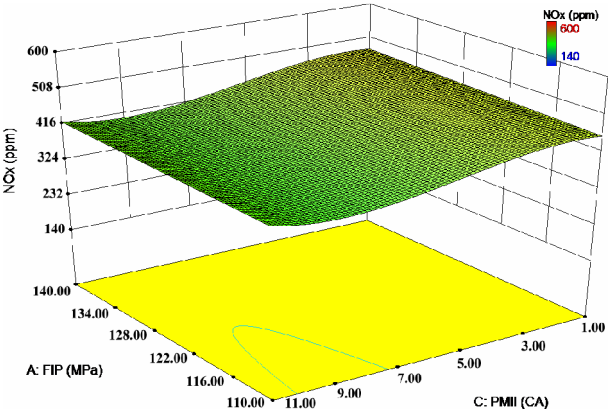

(a) Response surface

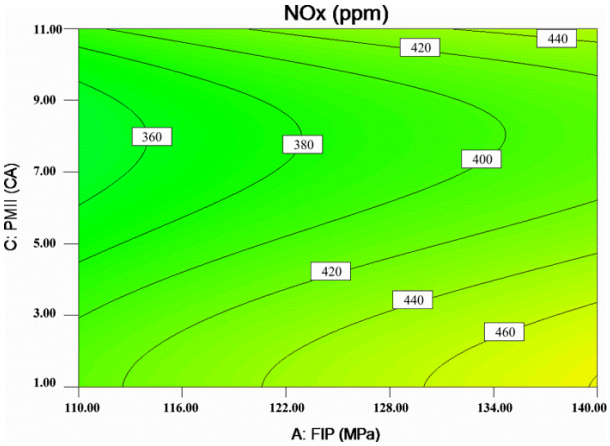

(b) Contour

Fig. 8. NO_X variations against FIP and PMII.

The interactive effect of FIP and PMII over NO_X concentration in exhaust gases at a constant SOI of 1.5 BTDC is demonstrated in Fig. 8. To better understand Fig. 8(a), a 2D contour map (Fig. 8(b)) was added. As shown, the increasing injection pressure strengthened the NO_X emissions. It is because higher fuel injection pressure improves the atomization and compresses the period of ignition delay, which makes faster combustion and higher in-cylinder gas temperature. Moreover, the presence of oxygen in J20 could also improve the combustion process. Due to superior combustion, under high temperatures nitrogen will react with oxygen to produce more NO_X emissions [29]. NO_X emission for J20 at 110 MPa was 346 ppm and it was 421 ppm at 140 MPa.

The effect of pilot-main injection intervals on NO_X emissions was significantly different than fuel injection pressure. As the intervals increased from 1 CA to 8.4 CA, NO_X emissions decreased gradually. The in-cylinder temperature and pressure were reduced by pilot injection; the ignition delay period extended to form the quite thinner air-fuel mixture, then the combustion temperature lowered, and NO_X emissions declined. However, NO_X emissions were slightly increased from 8.4 CA to 11 CA. As the pilot-main intervals further increased, the longer ignition delay period triggered strong

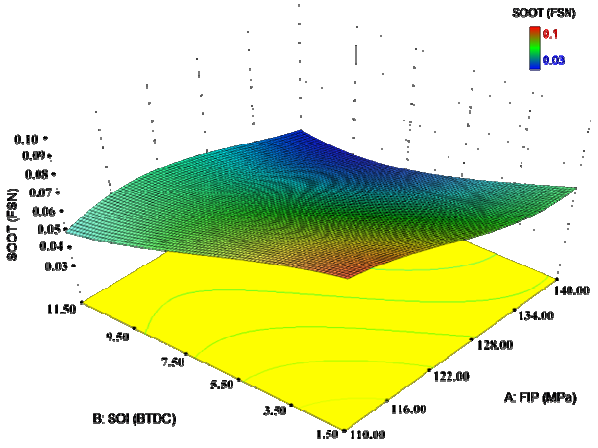

Fig. 9. Soot variations against FIP and SOI.

and rapid premixed combustion with high burning temperature, which promoted the production of NO_X emissions.

4.2 Soot emissions

The developed quadratic model of SOOT emissions as fitted based on RSM in terms of the experimental factors corresponded to:

$$\begin{aligned} SOOT &= 0.066\text{-}(2.412\text{E-}004)FIP\text{-}(5.492\text{E-}005)SOI \\ &+ 0.025PMII + (5.700\text{E-}006)FIP * SOI \text{ -}(1.042\text{E} \\ &\text{-}004)FIP * PMII\text{-}(4.026\text{E-}004)SOI * PMII\text{-}(7.500\text{E} \\ &\text{-}007)FIP^2 + (1.642\text{E-}005)SOI^2\text{-}(8.129\text{E-}004)PMII^2 . \end{aligned} \quad (5)$$

Fig. 9 shows SOOT emission characteristics as a function of injection pressure and injection timing at a constant PMII of 5 CA. As shown, decrease in SOOT emissions with increase in FIP was revealed. This is because of the presence of aromatic compounds and a lower carbon-to-hydrogen ratio in the blend [9]; on the other hand, the penetration of fuel spray increased, mixing of the fuel and air promoted, which resulted in premixed or rapid combustion stage of the combustion process. From Fig. 9 also, SOOT emissions decreased sharply with the increasing SOI. This could be mainly due to better combustion on the basis of more mixing time by early injection. However, when injection timing was retarded and it came near Top dead center (TDC) during the compression stroke, this provided shorter ignition delay and led to higher fuel fraction burning in diffusion combustion, thereby increasing SOOT emissions.

4.3 HC emissions

Quadratic response surface model for HC emissions based on multi-regression analysis was presented as Eq. (6):

$$\begin{aligned} HC &= 24.72 + 0.405FIP\text{-}11.324SOI - 7.063PMII \\ &+ 0.055FIP * SOI + 0.026FIP * PMII \\ &+ 1.213SOI * PMII\text{-}(5.125\text{E-}003)FIP^2 \\ &+ 0.893SOI^2 + 0.474PMII^2 . \end{aligned} \quad (6)$$

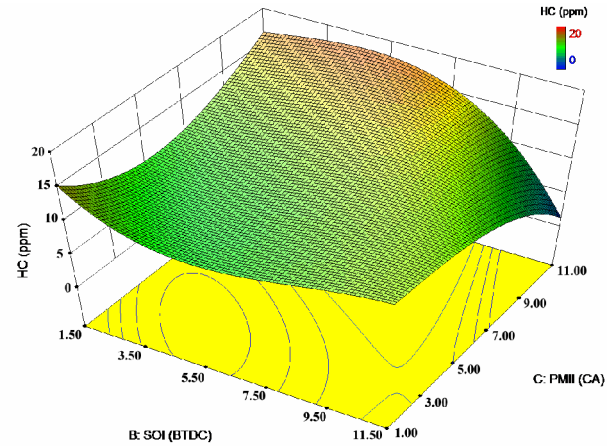

Fig. 10. HC variations against PMII and SOI.

The interactive effect of FIP and PMII over HC concentration in exhaust gases at a constant FIP of 130 MPa is demonstrated in Fig. 10. HC emission at 1.5 BTDC was remarkably higher than that at 5.5 and 11.5 BTDC due to inadequate mixing induced by extremely short ignition delay thanks to later injection. Note that HC emissions increased a little when SOI increased from 5.5 to 11.5 BTDC. The main reason might be that when SOI was over advanced, minute quantities of fuel were trapped in the cylinder wall. Fig. 10 also shows that HC emissions considerably decreased with the increase of PMII. In general, the increase of PMII causes increasing cylinder pressure and mean temperature before main combustion, leading to more complete combustion in the expansion stroke. Therefore, HC emissions decreased with the increase of PMII.

4.4 BTE and BSFC

The response surface quadratic model of BTE and BSFC in terms of the experimental results is given as Eqs. (7) and (8):

$$BTE = 0.229 + (9.552\text{E-}003)FIP + 0.018SOI - 0.29PMII - (4.619\text{E-}005)FIP * SOI + (2.323\text{E-}004)FIP * PMII - (5.283\text{E-}004)SOI * PMII - (9.374\text{E-}006)FIP^2 - (5.994\text{E-}004)SOI^2 - (7.035\text{E-}004)PMII^2 \quad (7)$$

$$BSFC = 266.675 - 0.282FIP - 3.462SOI - 0.970PMII + (8.996\text{E-}003)FIP * SOI - (2.477\text{E-}003)FIP * PMII + 0.080SOI * PMII + (9.300\text{E-}004)FIP^2 + 0.108SOI^2 + 0.068PMII^2. \quad (8)$$

The effects of injection pressure and injection timing on BTE (at a constant PMII of 5 CA) are shown in Fig. 11. As can be seen, BTE increased with increasing injection pressure. Higher injection pressure is beneficial to obtaining a fine atomization for enhanced penetration of fuel to promote vaporization in a short period and to gain better combustion efficiency [30].

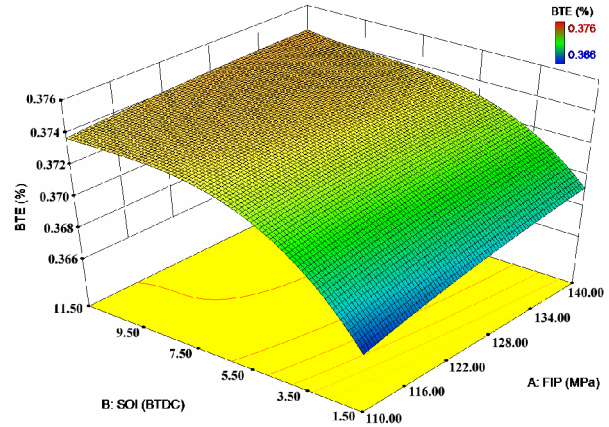

Fig. 11. BTE variations against FIP and SOI.

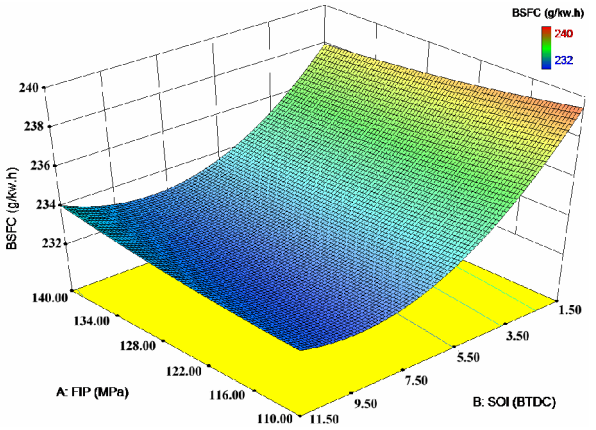

Fig. 12. BSFC variations against FIP and SOI.

Fig. 12 shows the RSM plot of BSFC for various FIP and SOI at a constant PMII of 3 CA. From Fig. 12, BSFC increased as the injection timing was retarded from 11.5 BTDC to 1.5 BTDC. The increasing of SOI caused increase in average BSFC by 2.16 %.

4.5 Optimization

Optimization is one of the most essential procedures in analysis of multi-target experiments. The above discussions on the impact of FIP, SOI and PMII on performances and emissions indicated that:

(1) Advanced injection timings led to lower HC and SOOT emissions, higher BTE;

(2) Higher injection pressures resulted in high values of NO_X with lower SOOT and BSFC;

(3) Larger PMII caused lower NO_X and HC emissions.

As there was a trade-off between NO_X, SOOT, HC, BTE and BSFC, it was crucial to optimize the FIP, SOI and PMII with the target of minimizing the BSFC and emissions and maximizing the BTE. The criterion for the majorization such as the target set for each response (NO_X, SOOT, HC, BTE and

Table 6. Optimization criteria.

Parameter or response	Lower limits	Upper limits	Weight		Importance	Goal	Desirability
			Upper	Lower			
FIP (MPa)	110	140	1	1	3	In range	1
SOI (BTDC)	1.5	11.5	1	1	3	In range	1
PMII (CA)	1	11	1	1	3	In range	1
NO_X (ppm)	298.32	800.38	0.1	1	5	Minimize	0.983
SOOT (FSN)	0.004	0.128	0.1	1	5	Minimize	0.952
HC (ppm)	11.23	39.74	0.1	1	5	Minimize	0.975
BSFC (g/kW h)	232.053	251.49	0.1	1	5	Minimize	0.982
BTE (%)	0.34703	0.375706	1	0.1	5	Maximize	0.993
Combined	-	-			-	-	0.967

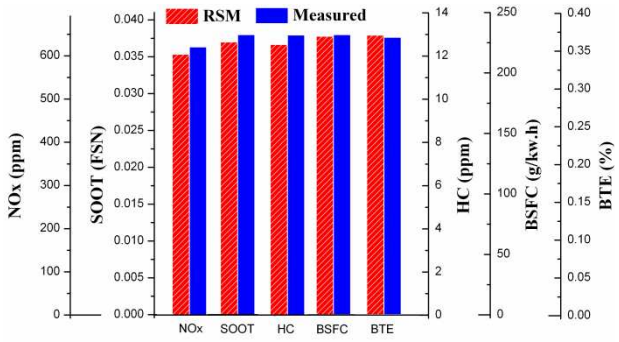

Fig. 13. RSM and experimental results.

BSFC), lower and upper limits used, weights used and importance of the factors is shown in Table 6. Optimization was carried out by using the desirability profile and its functions. In desirability based approach, various best solutions were obtained. The maximum desirability of 0.967 was chosen at the following fuel supply parameters such as 134.11 MPa of FIP, 6.4 BTDC of SOI, and 5.8 CA of PMII, which could be considered as the optimum parameters for the test engine having 603.44 ppm of NO_X, 0.037 FSN of SOOT, 12.73 ppm of HC, 233.26 g/kW.h of BSFC and 37.31 % of BTE.

For validating the optimal solution, experiments were conducted at the optimum fuel supply parameters. Test results were 620.62 ppm of NO_X, 0.038 FSN of SOOT, 13.17 ppm of HC, 234.58 g/kW h of BSFC and 37.05 % of BTE. The relative errors were 2.84 %, 2.70 %, 3.46 %, 0.56 %, -0.69 %, respectively. Fig. 13 shows the comparison of RSM and experimental results. The validation results revealed that the RSM models developed were extremely reliable as the percentages of error in predictions were in a good fit.

5. Conclusion

The following were the conclusions arrived on performing several tests in a diesel engine fueled with J20 by varying the fuel injection pressure, start of injection timing and pilot-main injection intervals at different levels concurrently:

- The design of experiments based on RSM was extremely beneficial to design the experiment. Moreover, the statistical analysis contributed to identify the significant parameters which are most influencing the emission and performance characteristics. This design of experiment highly reduced the time and cost required by minimizing the number of tests to be performed and represented statistically proven models for all the responses.
- Increase in injection pressure increases BTE with lesser BSFC for all SOI and PMII of the engine.
- Advancing the injection timing from 1.5 BTDC to 11.5 BTDC helped to reduce the SOOT and HC with increase in BTE.
- At moderate pilot-main injection intervals, lesser NO_X with low HC was founded.
- At optimum injection parameters viz. FIP of 134.11 MPa, SOI of 6.4 BTDC with PMII of 5.8 CA, the values of the NO_X, SOOT, HC, BSFC and BTE were found to be 603.44 ppm, 0.037 FSN, 12.73 ppm, 233.26 g/kW h and 37.31 %, respectively. Maximum relative error of RSM results with experiment data was less than 4 %.

Acknowledgment

The authors would like to acknowledge the contribution of Project supported by the Natural Science Foundation of Jiangsu Province, China (Grant No. BK20150520); Graduate student innovation fund project of Jiangsu province (KYLX16_0890); The projects of 'Six talent peak' (grant number 2014-ZBZZ-014); The Priority Academic Program Development of Jiangsu Higher Education Institutions (PAPD); Senior professionals scientific research fund project of Jiangsu University (13JDG104); China Postdoctoral Science Foundation (2014M560400).

Nomenclature

RSM : Response surface methodology
FIP : Fuel injection pressure
SOI : Start of injection timing

PMII : Pilot-main injection intervals
NO_X : Nitrogen oxide
PM : Particulate matter
ESC : European steady state cycle
BSFC : Brake specific fuel consumption

References

[1] G. Karavalakis, K. C. Johnson, M. Hajbabaei and T. D. Durbin, Application of low-level biodiesel blends on heavy-duty (diesel) engines: Feedstock implications on NO_X and particulate emissions, *Fuel*, 181 (2016) 259-268.

[2] C. Klessmann, A. Held, M. Rathmann and M. Ragwitz, Status and perspectives of renewable energy policy and deployment in the European Union—What is needed to reach the 2020 targets?, *Energy Policy*, 39 (2011) 7637-7657.

[3] G. Knothe, A technical evaluation of biodiesel from vegetable oils vs. algae. Will algae-derived biodiesel perform?, *Cheminform*, 43 (2011) 3048-3065.

[4] R. Luque, J. C. Lovett, B. Datta, J. Clancy, J. M. Campelo and A. A. Romero, Biodiesel as feasible petrol fuel replacement: a multidisciplinary overview, *Energy & Environmental Science*, 3 (2010) 1706-1721.

[5] A. S. Silitonga, H. H. Masjuki, T. M. I. Mahlia, H. C. Ong, F. Kusumo, H. B. Aditiya and N. N. N. Ghazali, Schleichera oleosa L oil as feedstock for biodiesel production, *Fuel*, 156 (2015) 63-70.

[6] M. M. Rahman, M. H. Hassan, M. A. Kalam, A. E. Atabani, L. A. Memon and S. M. A. Rahman, Performance and emission analysis of Jatropha curcas and Moringa oleifera methyl ester fuel blends in a multi-cylinder diesel engine, *Journal of Cleaner Production*, 65 (2014) 304-310.

[7] J. Jeon and S. Park, Effects of pilot injection strategies on the flame temperature and soot distributions in an optical CI engine fueled with biodiesel and conventional diesel, *Applied Energy*, 160 (2015) 581-591.

[8] A. Sanjid, H. Masjuki, M. Kalam, S. A. Rahman, M. Abedin and S. Palash, Production of palm and jatropha based biodiesel and investigation of palm-jatropha combined blend properties, performance, exhaust emission and noise in an unmodified diesel engine, *J. of Cleaner Production*, 65 (2014) 295-303.

[9] G. Gonca and E. Dobrucali, Theoretical and experimental study on the performance of a diesel engine fueled with diesel–biodiesel blends, *Renewable Energy*, 93 (2016) 658-666.

[10] S. K. Nayak, S. K. Nayak, P. C. Mishra and S. Tripathy, Influence of compression ratio on combustion characteristics of a VCR engine using Calophyllum inophyllum biodiesel and diesel blends, *J. of Mechanical Science and Technology*, 29 (9) (2015) 4047-4052.

[11] I. M. Monirul, H. H. Masjuki, M. A. Kalam, M. H. Mosarof, N. W. M. Zulkifli, Y. H. Teoh and H. G. How, Assessment of performance, emission and combustion characteristics of palm, jatropha and Calophyllum inophyllum biodiesel blends, *Fuel*, 181 (2016) 985-995.

[12] A. Nalgundwar, B. Paul and S. K. Sharma, Comparison of performance and emissions characteristics of DI CI engine fueled with dual biodiesel blends of palm and jatropha, *Fuel*, 173 (2016) 172-179.

[13] O. Hwaichyuan, H. H. Masjuki, T. M. I. Mahlia, A. S. Silitonga, W. T. Chong and K. Y. Leong, Optimization of biodiesel production and engine performance from high free fatty acid Calophyllum inophyllum oil in CI diesel engine, *Energy Conversion & Management*, 81 (2014) 30-40.

[14] K. Cheikh, A. Sary, L. Khaled, L. Abdelkrim and T. Mohand, Experimental assessment of performance and emissions maps for biodiesel fueled compression ignition engine, *Applied Energy*, 161 (2016) 320-329.

[15] D. Deshmukh, A. M. Mohan, T. N. C. Anand and R. V. Ravikrishna, Spray characterization of straight vegetable oils at high injection pressures, *Fuel*, 97 (2012) 879-883.

[16] E. Torres-Jimenez, M. Kegl, R. Dorado and B. Kegl, Numerical injection characteristics analysis of various renewable fuel blends, *Fuel*, 97 (2012) 832-842.

[17] H. Taghavifar, H. Taghavifar, A. Mardani, A. Mohebbi and S. Khalilarya, A numerical investigation on the wall heat flux in a DI diesel engine fueled with n-heptane using a coupled CFD and ANN approach, *Fuel*, 140 (2015) 227-236.

[18] J. B. Hirkude and A. S. Padalkar, Performance optimization of CI engine fuelled with waste fried oil methyl ester-diesel blend using response surface methodology, *Fuel*, 119 (2014) 266-273.

[19] A. Abuhabaya, J. Fieldhouse and D. Brown, The effects of using biodiesel on CI (compression ignition) engine and optimization of its production by using response surface methodology, *Energy*, 59 (2013) 56-62.

[20] G. Khoobbakht, G. Najafi and M. Karimi, Optimization of operating factors and blended levels of diesel, biodiesel and ethanol fuels to minimize exhaust emissions of diesel engine using response surface methodology, *Applied Thermal Engineering*, 99 (2016) 1006-1017.

[21] A. E. Dhole, R. B. Yarasu, D. B. Lata and S. S. Baraskar, Mathematical modeling for the performance and emission parameters of dual fuel diesel engine using hydrogen as secondary fuel, *International J. of Hydrogen Energy*, 39 (2014) 12991-13001.

[22] T. Lee and R. D. Reitz, Response surface method optimization of a high-speed direct-injection diesel engine equipped with a common rail injection system, *J. of Engineering for Gas Turbines and Power*, 125 (2003) 541-546.

[23] Y. Meng, X. Wang, Z. Wu, S. Wang and T. M. Young, Optimization of cellulose nanofibrils carbon aerogel fabrication using response surface methodology, *European Polymer J.*, 73 (2015) 137-148.

[24] Y. Xie, L. Chen and L. Rui, Oxidation of AOX and organic compounds in pharmaceutical wastewater in RSM-optimized-Fenton system, *Chemosphere*, 155 (2016) 217.

[25] M. A. Bezerra, R. E. Santelli, E. P. Oliveira, L. S. Villar and L. A. Escaleira, Response surface methodology (RSM) as a tool for optimization in analytical chemistry, *Talanta*, 76

(2008) 965-977.

[26] T. Zhao, Y. Shi, X. Lin and T. Huang, Optimization of abrasive flow polishing process parameters for static blade ring based on response surface methodology, *J. of Mechanical Science and Technology*, 30 (3) (2016) 1085-1093.

[27] O. Dogan, F. Karpat, C. Yuce, N. Kaya, N. Yavuz and H. Sen, A novel design procedure for tractor clutch fingers by using optimization and response surface methods, *J. of Mechanical Science and Technology*, 30 (6) (2016) 2615-2625.

[28] M. Pandian, S. P. Sivapirakasam and M. Udayakumar, Investigation on the effect of injection system parameters on performance and emission characteristics of a twin cylinder compression ignition direct injection engine fuelled with pongamia biodiesel–diesel blend using response surface methodology, *Applied Energy*, 88 (2011) 2663-2676.

[29] C. S. Aalam, C. Saravanan and B. P. Anand, Impact of high fuel injection pressure on the characteristics of CRDI diesel engine powered by mahua methyl ester blend, *Applied Thermal Engineering*, 106 (2016) 702-711.

[30] J. I. J. Lalvani, M. Parthasarathy, B. Dhinesh and K. Annamalai, Pooled effect of injection pressure and turbulence inducer piston on performance, combustion, and emission characteristics of a DI diesel engine powered with biodiesel blend, *Ecotoxicology And Environmental Safety*, 134 (2016) 336-34.

Huaping Xu received the M.E. in Marine Engineering from Jiangsu University of Science and Technology, Zhenjiang, China, in 2009. In 2014, he joined Jiangsu University, Zhenjiang, China, as a doctoral student. His research interests and activities have included performance optimization of internal combustion engine and laser diagnostics in combustion.

Bifeng Yin received the B.S., M.E. and Ph.D. in Electrical Engineering from Jiangsu University, Zhenjiang, China, in 1998, 2001, and 2011, respectively. He is currently a Professor of Power Machinery and Engineering with Jiangsu University. His research interests and activities have included tribology, fuel spray and atomization, combustion and emissions control.